Revision

Interfacial Electron Shuttling Processes Across Kolliphor®EL Monolayer Grafted Electrodes

Khadijeh Nekoueian [a,b,c], Christopher E. Hotchen [a], Mandana Amiri [b], Mika Sillanpää [c], Geoffrey W. Nelson [d], John S. Foord [e], Philip Holdway [f], Antoine Buchard [a], Stephen C. Parker [a], and Frank Marken [a]*

[a] *Department of Chemistry, University of Bath, Bath BA2 7AY, UK*
[b] *Department of Chemistry, University of Mohaghegh Ardabili, Ardabil, Iran*
[c] *Laboratory of Green Chemistry, School of Engineering Science, Lappeenranta University of Technology, Sammonkatu 12, FI-50130 Mikkeli, Finland*
[d] *Imperial College London, Department of Materials, Royal School of Mines, Exhibition Road, London, SW7 2AZ, UK*
[e] *Chemistry Research Laboratories, Oxford University, South Parks Road, Oxford OX1 3TA, UK*
[f] *Department of Materials, Oxford University, Begbroke Science Park, Begbroke Hill, Oxford OX5 1PF, UK*

Proofs to F. Marken
Email f.marken@bath.ac.uk

Abstract

Covalently grafted Kolliphor®EL (a poly-ethylene-glycol based "transporter molecule" for hydrophobic water-insoluble drugs; MW ca. 2486; diameter ca. 3-5 nm) at the surface of a glassy carbon electrode strongly affects the rate of electron transfer for aqueous redox systems such as $Fe(CN)_6^{3-/4-}$. XPS data confirm mono-layer grafting after electrochemical anodisation in pure Kolliphor®EL. Based on voltammetry and impedance measurements, the charge transfer process for the $Fe(CN)_6^{3-/4-}$ probe molecule is completely blocked after Kolliphor®EL grafting and in the absence of a "guest". However, in the presence of low concentrations of suitable ferrocene derivatives as "guests", mediated electron transfer across the mono-layer via a "shuttle mechanism" is observed. The resulting amplification of the ferrocene electroanalytical signal is investigated systematically and compared for 5 ferrocene derivatives. The low concentration electron shuttle efficiency decreases in the sequence dimethylaminomethyl-ferrocene > n-butyl-ferrocene > ferrocene-dimethanol > ferrocene-acetonitrile > ferrocene-acetic acid.

Keywords: chremophor, pegylation, amplification, voltammetry, tunneling, sensor.

1. Introduction

Surface modified electrodes are widely used in sensors[1] and in film electrodes.[2,3,4] Covalent grafting of a mono-layer onto carbon electrode surfaces can be achieved by diazonium methods,[5,6] by "click" chemistry,[7] by amide chemical attachment,[8] or by many other similar processes.[9] The electrochemical surface modification offers the advantage (over chemical processes) of potential control and optimization to achieve a well-defined mono-layer coverage. A wide range of often radical-based intermediates are known to attach spontaneously to carbon electrode surfaces.[10,11] We have recently adapted a methodology introduced by Maeda and coworkers[12,13] to attach poly(ethylene-glycol) (or PEG) derivatives to glassy carbon and boron-doped diamond electrode surfaces.[14] An anodic treatment was developed to allow mono-layer attachment of PEGs with a resulting structure-dependent retardation of the rate of heterogeneous electron transfer. In this study a pegylated castor oil derivative, Kolliphor®EL (CAS number 61791-12-6, MW ca. 2486 g mol^{-1}; see Figure 1) is selected to demonstrate this anodic grafting process for a more complex molecule.

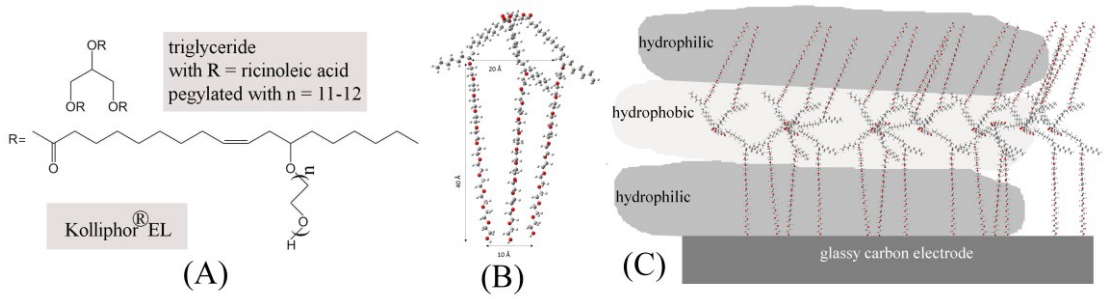

Figure 1. (A) Molecular structure of the main component in Kolliphor®EL and (B) 3D rendering (GaussView 5.0) showing the approximate diameter of 3-5 nm. (C) Schematic drawing of a Kolliphor®EL mono-layer with a hydrophobic region due to the triglyceride.

For pegylated molecules like Kolliphor®EL the hydroxyl end groups are sensitive to oxidation with radical intermediates likely to bind to the carbon electrode surface.[15] Kolliphor®EL (see Figure 1) as a pegylated castor oil derivative is often employed as medicinal additive or "drug carrier" reagent[16] to allow water-insoluble drug molecules to be "solubilized" and carried to the location of action. Based on this, it could introduce interesting new properties (with a hydrophobic layer, Figure 1C) to the modified carbon electrode surface. Similarly, pegylation is widely used to impose hydrophilic character to surfaces, particles, and molecules.[17] In this study the Kolliphor®EL surface layer is employed (i) as a barrier to electron transfer and (ii) as a host film to allow hydrophobic reagents to bind and enhance or "amplify" interfacial electron transfer.

Amplification of electroanalytical signals is often desirable and possible, for example, by (i) direct feedback in generator-collector electrode devices[18] and (ii) in catalytic processes where an enzyme[19] or nano-particle catalyst[20] is employed to enhance the analytical response. Here, amplification is achieved simply based on a difference in the rate of heterogeneous electron transfer for two redox systems. Figure 2 shows a schematic drawing of the electrode surface with a layer of Kolliphor®EL immobilized. The direct electron transfer to the $Fe(CN)_6^{3-/4-}$ redox system is suppressed, but the presence of a "shuttle" molecule such as ferrocene (Fc) can be employed to "restore" electron transfer. Very low concentrations of ferrocene can therefore be detected as relatively large "amplified" currents.

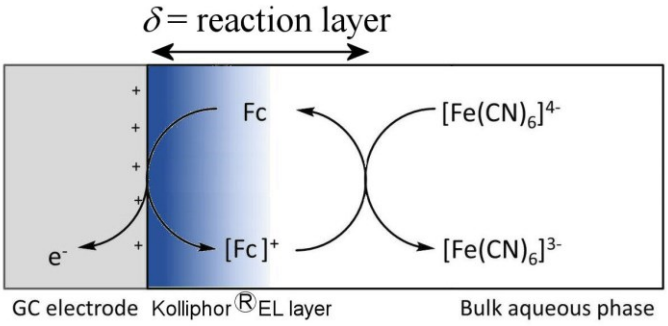

Figure 2. Schematic drawing of the "amplification" mechanism for the low concentration ferrocene (Fc) redox process in the presence of the "suppressed" $Fe(CN)_6^{3-/4-}$ electron transfer.

Here, the Maeda method is employed to produce a Kolliphor®EL mono-layer on a glassy carbon electrode surface. It is shown that this results in a dramatic decrease in the rate of heterogeneous electron transfer for aqueous $Fe(CN)_6^{3-/4-}$. Ferrocene derivatives are then compared with respect to their "shuttle ability" for electrons to pass through the Kolliphor®EL layer. A quantitative study reveals the structural parameters that govern the shuttle process. Future applications are envisaged in the amplification (or modulation) of other types of electron transfer processes, e.g. in analytical drug or explosives detection applications.

2. Experimental

2.1. Chemical Reagents

Kolliphor®EL (CAS number 61791-12-6; MW ca. 2450 g mol^{-1}; previously also known as Chremophor EL; Aldrich) is a pegylated castor oil derivative (Figure 1). Lithium perchlorate ($LiClO_4$, Sigma-Aldrich, ≥ 95 %, ACS reagent) was used as background electrolyte in neat Kolliphor®EL solutions. Ferrocene dimethanol ($Fc(MeOH)_2$, Aldrich, 98 %), ferrocene acetic acid (FcAcOH, Aldrich, 98 %),

ferrocene acetonitrile (FcMeCN, Aldrich), *n*-butyl ferrocene (BuFc, Alfa Aesar, 98 %, oil), *N*,*N'*-dimethylaminomethyl ferrocene ($MeFcNMe_2$, TCI Europe, oil), potassium ferrocyanide(II) ($K_4Fe(CN)_6$, Fisons, 98 %) and potassium ferricyanide(III) ($K_3Fe(CN)_6$, Aldrich, 99+ %) were used as redox species in aqueous solutions containing 0.1 M potassium nitrate (KNO_3, Sigma-Aldrich, ≥ 99.0 %) as background electrolyte.

2.2. Instrumentation

All electrochemical measurements were performed using an Ivium Compactstat 104 Model B08084 (Ivium Technologies NL). A step potential of 1 mV was used in cyclic voltammetry experiments. Electrochemical impedance spectroscopy (EIS) was performed at open circuit potential (OCP = 0.19 V vs. SCE) in a 5 mM $Fe(CN)_6^{3-}$ and 5 mM $Fe(CN)_6^{4-}$ containing 0.1 M KNO_3 solution with an amplitude of 10 mV. The frequency was varied from 10 kHz to 0.01 Hz. Equivalent circuit data fitting was carried out using ZView software.

X-ray photoelectron spectroscopy (XPS) experiments were performed using a Thermo K Alpha (Thermo Scientific) spectrometer (operating at ≈ 10^{-8} – 10^{-9} Torr), a 180° double focusing hemispherical analyzer running in constant analyzer energy (CAE) mode with a 128-channel detector. A mono-chromated Al Kα radiation source (1486.7 eV) was used. Peak fitting was performed with XPS Peak Fit (v. 4.1) software using Shirley background subtraction. Peaks were referenced to the adventitious carbon C1s peak (284.6 eV) and peak areas were normalized to the photoelectron cross-section of the F1s photoelectron signal using atomic sensitivity factors.[21]

2.3. Procedure for Kolliphor®EL Grafting

Kolliphor®EL is a viscous liquid and can be employed directly as a solvent in electrochemical experiments after addition of suitable electrolyte. Here, a solution of 20 mM $LiClO_4$ in Kolliphor®EL is employed for the electrode modification process. A 3 mm diameter glassy carbon electrode is placed into this solution with +1.6 V vs. SCE applied for 20 minutes (optimized previously[14]). The electrode is then rinsed with water and dried. The extent of surface modification is apparent from XPS data for two independently prepared samples K1 and K2 (Figure 3).

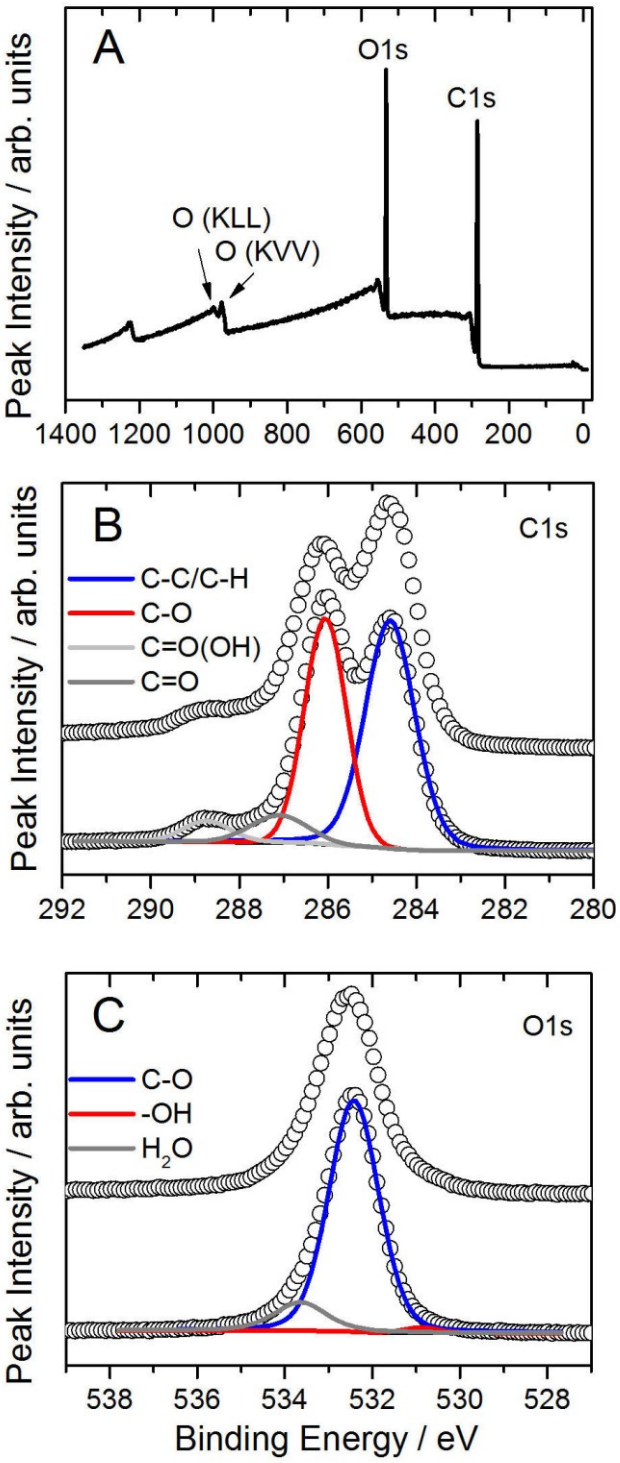

Figure 3. Representative survey XPS spectra of Kolliphor®EL modification of glassy carbon (A); XPS core level spectra of modified substrate: C1s (B) and O1s (C). Representative curve fits (see experimental) are shown for C1s and O1s and for two independently investigated samples (see dotted lines, K1 bottom, K2 above, see Table 1).

Survey spectra show photoelectron signals from contaminant-free surfaces containing C and O (Figure 3A). The C1s photoelectron signals show evidence for a PEG-like interface. The C1s spectra associated with Kolliphor®EL samples K1 and K2 are shown in Figure 3B. The spectra could be fitted (see experimental) into four chemical environments: adventitious carbon and hydrocarbon (284.6 eV), ether (C-O, ≈ 286.1 eV), carbonyl (C=O, ≈ 287.1 eV) and carboxyl (C=O(OH), ≈ 288.1 eV).[22] The O1s photoelectron signal in Figure 3C was curve fitted using the model established by Schlapak *et al.*[23] as follows: hydroxyl (-OH, ≈ 531 eV), ether (C-O, ≈ 532.2 eV), water (H_2O, ≈ 533.5 eV). The above spectra are consistent with PEG-like surface chemistry, with contribution from C-O from repeated poly(ethylene-glycol) units dominating the observed photoelectron signal. The presence of hydroxyl and water O1s signals suggests that trace water is present within the interface, which is to be expected as water binds strongly to PEG. XPS data are summarized in Table 1. Variation between samples K1 and K2 suggest some position dependence and/or sample-to-sample variability. Key changes in comparison to the bare glassy carbon surface are (i) an increase in O1s/C1s ratio mainly due to C-O, (ii) and increase in C1s for C-O, and (iii) an increase in O1s for C-O.

Table 1. XPS ratios and surface composition for two independently investigated samples with Kolliphor®EL mono-layer (K1 and K2) and a bare glassy carbon substrate (GC). Peak integration methods based on literature models for C1s[17] and O1s[18] were employed.

		C1s composition / %				**O1s composition / %**		
Sample	**O1s/C1s**	**C-C**	**C-O**	**C=O**	**C=O(OH)**	**OH**	**H_2O**	**C-O**
K1	2.94	39.1	50.2	6.4	4.3	1.3	12.6	86.1
K2	3.12	54.7	33.8	4.8	6.7	5.3	12.8	81.9
GC	1.29	66	11	11	8	12	33	55

3. Results and Discussion

3.1. Kolliphor®EL Grafting Affects Heterogeneous Electron Transfer Kinetics

Kolliphor®EL is medicinal formulation additive and a "transporter" molecule for drugs and poorly water-soluble materials.[16] It is employed here when grafted as a mono-layer directly onto glassy carbon electrode surfaces. Although only mono-layer deposition occurs, a dramatic effect of this surface modification is detected on the heterogeneous electron transfer for the $Fe(CN)_6^{3-/4-}$ redox system (equation 1).

$$Fe(CN)_6^{3-} + e^- \rightleftharpoons Fe(CN)_6^{4-} \qquad (1)$$

This redox system is often employed to probe surface modification effects[24] and here it is shown to be highly sensitive to Kolliphor®EL grafts. Figure 4A displays cyclic voltammetry data first for the unmodified glassy carbon electrode and then for the Kolliphor®EL modified electrode. The heterogeneous electron transfer to $Fe(CN)_6^{3-/4-}$ is close to completely suppressed within the potential range investigated here. The approximate diameter of the Kolliphor®EL molecules is 1 nm (see Figure 1), which appears to be sufficient to essentially "switch off" the heterogeneous electron transfer. A gentle polish is sufficient to reverse the effect.

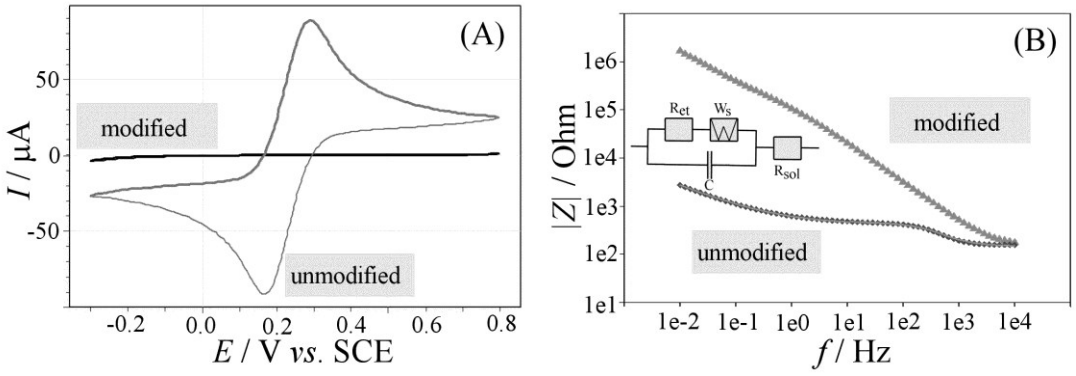

Figure 4. (A) Cyclic voltammograms (scan rate 50 mVs^{-1}) for a 3 mm glassy carbon electrode immersed in aqueous 5 mM $Fe(CN)_6^{3-}$, 5 mM $Fe(CN)_6^{4-}$, and 0.1 M KNO_3 before and after Kolliphor®EL grafting. (B) Impedance data for the same system at the equilibrium potential.

The experiment was repeated with impedance analysis to explore the effect in the time domain. Figure 4B shows impedance data for unmodified and modified electrodes. For the unmodified electrode a conventional Randles circuit model (see inset in Figure 4B) was employed (the line of best fit overlays data in Figure 4B) giving R_{sol} = 154 Ω, R_{et} = 266 Ω, C = 1.8 μF, W_P = 0.5, W_T = 107 and W_R = 6310 Ω. For the Kolliphor®EL modified electrode the impedance response is associated mainly with capacitive charging (see Figure 4B) with R_{sol} and C values similar to those for the unmodified electrode. However, a good fit was not possible. This is believed to be due to low frequency data revealing additional complexity, which could be due to some remaining porosity in the grafted layer and associated with some electron transfer at frequencies below 1 Hz. In summary, the Kolliphor®EL grafting strongly suppresses electron transfer to $Fe(CN)_6^{3-/4-}$ and it is now possible to introduce "guest molecules" to explore "shuttle" effects and changes in electron transfer.

3.2. Kolliphor®EL Grafting Affecting Heterogeneous Electron Transfer Kinetics: Ferrocene Mediators

In contrast to the dramatic change in the rate of heterogeneous electron transfer observed for the hydrophilic $Fe(CN)_6^{3-/4-}$, the rates of electron transfer for many more hydrophobic ferrocene derivatives are potentially less sensitive to the surface modification. This is consistent here with the less hydrated and more hydrophobic ferrocene derivatives penetrating into the Kolliphor®EL film and effectively operating as "electron shuttles" between the electrode surface and the solution redox species (such as. $Fe(CN)_6^{3-/4-}$). The "shuttle efficiency" is investigated for 5 different ferrocene derivatives.

Ferrocene-dimethanol (see Figure 5) is modestly water soluble and employed here as an "electron shuttle" at 0, 5, 10, and 50 μM concentrations to lower the electron transfer impedance between the electrode and $Fe(CN)_6^{3-/4-}$. The voltammetric signal at the Kolliphor®EL modified glassy carbon increases from no signal to 42 μA peak current (see Figure 5A), which is close to the diffusion limited value for the $Fe(CN)_6^{3-/4-}$ species (compare Figure 4A). The underlying voltammetric signal for the ferrocene-dimethanol itself remains insignificant on this scale and is not detected in this experiment. Only the "amplified" net-current for the $Fe(CN)_6^{3-/4-}$ redox system is detected.

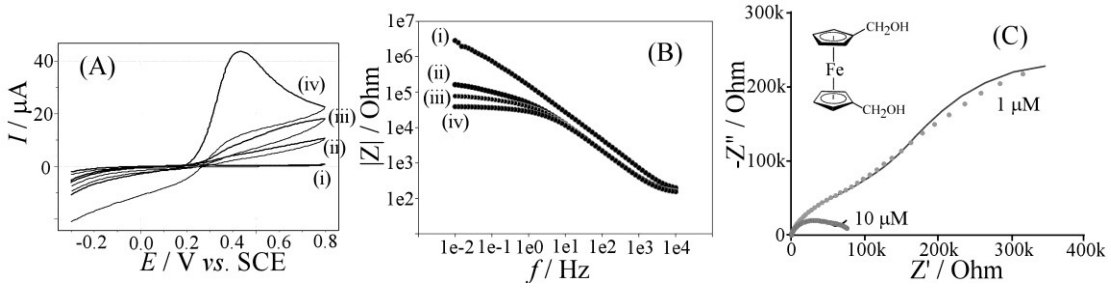

Figure 5. (A) Cyclic voltammograms (scan rate 50 mVs^{-1}) for a 3 mm glassy carbon electrode immersed in aqueous 5 mM $Fe(CN)_6^{3-}$, 5 mM $Fe(CN)_6^{4-}$, and 0.1 M KNO_3 with addition of (i) 0, (ii) 5, (iii) 10, (iv) 50 µM ferrocene-dimethanol. (B) Impedance data for this system at equilibrium potential. (C) Nyquist plot with simulation model data (line) and experimental data (dots) for 1 µM and 10 µM ferrocene-dimethanol.

The "electron shuttle" effect is seen also in the impedance data (Figure 5B), where a significant change in the lower frequency range (below 10 Hz) is consistent with the flow of Faradaic current catalyzed by the ferrocene-dimethanol mediator. Figure 5C shows two sets of experimental (dots) impedance data with simulation data (line), which will be discussed below.

When employing ferrocene-acetonitrile as the "electron shuttle" (see Figure 6A), a similar change in the cyclic voltammetry peak current is observed. However, the peak currents for oxidation (Figure 6A) appear lower compared to data in Figure 5A with less cathodic current observed on the reverse scan. Table 2 summarises some data for voltammetric features (and impedance data, *vide infra*) observed for the different ferrocene derivatives in experiments at Kolliphor®EL modified glassy carbon electrodes. The reversible potential for $Fe(CN)_6^{4-/3-}$ here is 0.19 V vs. SCE and it can be seen that for all ferrocene derivatives a higher E_0 (consistent with less driving force for reduction) makes the "amplification" process asymmetric with less driving force for the cathodic signal. The magnitude of the anodic peak signal is likely to be

correlated also to the peak-to-peak separation ΔE_p (indicative slower electron transfer kinetics, see Table 2). Therefore, the lower mediated oxidation peaks for ferrocene-acetonitrile (Figure 6) and for ferrocene-acetic acid (Figure 7), when comparing to other ferrocene derivatives, are likely to be linked here primarily to the slower kinetics of electron transfer (consistent with a wider peak-to-peak separation) limiting the electron shuttle rate.

Table 2. Summary of data from voltammetry and impedance spectroscopy. Solution with 50 μM ferrocene derivative, 5 mM $Fe(CN)_6^{3-}$, 5 mM $Fe(CN)_6^{4-}$, in 0.1 M KNO_3 (scan rate 50 mVs^{-1}). Impedance data relate to a Randles circuit (see text) with W_P = 0.5 and $\delta_{app} = (W_T \times D)^{1/2}$ with $D = 0.6 \times 10^{-9}$ m^2s^{-1} as an approximate value[25] used for all ferrocene derivatives.

	E_0 [a] / V vs. SCE	ΔE_p [a] / V	[Fc] / μM	R_{sol} /Ω	R_{et} /Ω	W_R [b] / kΩ	W_T [b] / s	CPE_T / μF	CPE_P	δ_{app} / μm
ferrocene-dimethanol	0.28	0.11	1	127	9177	524	38.9	2.84	0.796	153
			10	134	5073	268	5.16	2.78	0.798	56
ferrocene-acetonitrile	0.21	0.22	1	137	2958	690	82.5	2.39	0.816	222
			10	150	5332	635	67.3	2.30	0.835	201
ferrocene-acetic acid	0.20	0.22	1	123	7815	1720	393	2.32	0.843	486
			10	132	6063	89	11.8	2.58	0.832	84
dimethylamino-methyl-ferrocene	0.27	0.10	1	135	6180	123	2.82	4.01	0.795	41
			10	138	3092	335	19.0	2.69	0.838	107
n-butyl-ferrocene	0.22	0.04	1	130	6557	139	8.14	1.82	0.789	70
			10	127	1117	127	222	3.94	0.743	365

[a] obtained from cyclic voltammograms of 50 μM solution of ferrocene derivative in 0.1 M KNO_3 at a Kolliphor®EL modified glassy carbon electrode. Note that signals in particular for ferrocene-acetonitrile, dimethylaminomethyl-ferrocene, and n-butyl-ferrocene are complicated by the interaction with the electrode surface

[b] a short Warburg element was selected to reflect the electron transfer to $Fe(CN)_6^{3-/4-}$

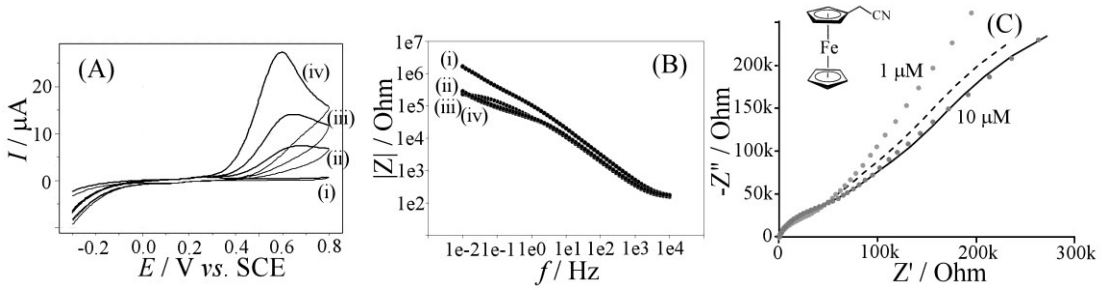

Figure 6. (A) Cyclic voltammograms (scan rate 50 mVs^{-1}) for a 3 mm glassy carbon electrode immersed in aqueous 5 mM $Fe(CN)_6^{3-}$, 5 mM $Fe(CN)_6^{4-}$, and 0.1 M KNO_3 with addition of (i) 0, (ii) 5, (iii) 10, (iv) 50 μM ferrocene-acetonitrile. (B) Impedance data for this system at equilibrium potential. (C) Nyquist plot with simulation model data (dashed and line) and experimental data (dots) for 1 μM and 10 μM ferrocene-acetonitrile.

Next, ferrocene-acetic acid is employed as the "electron shuttle" (Figure 7) and similar trends are observed. However, the suppression of the oxidation peaks is more pronounced. Based on data in Table 2 very similar behavior for ferrocene-acetonitrile and ferrocene-acetic acid could be predicted, but additional electrostatic repulsion (at neutral pH) of the negatively charged ferrocene-acetate and the $Fe(CN)_6^{3-/4-}$ redox system is likely to further limit the "electron shuttle" efficiency. The impedance at the equilibrium potential shows very similar features compared to the data for ferrocene-acetonitrile with somewhat lower impedance for higher ferrocene mediator concentration.

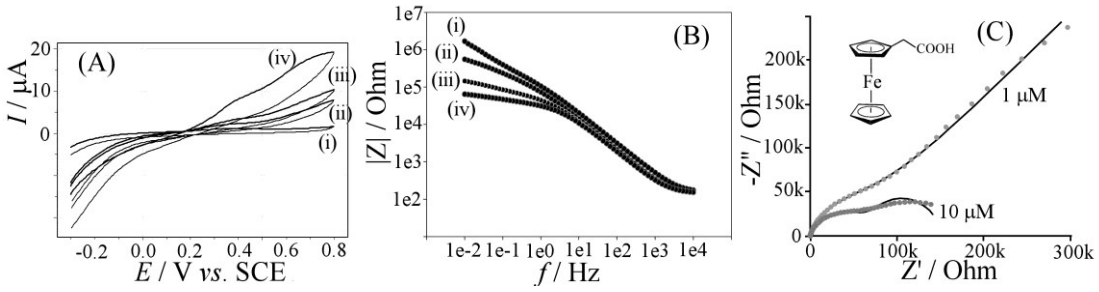

Figure 7. (A) Cyclic voltammograms (scan rate 50 mVs^{-1}) for a 3 mm glassy carbon electrode immersed in aqueous 5 mM $Fe(CN)_6^{3-}$, 5 mM $Fe(CN)_6^{4-}$, and 0.1 M KNO_3 with addition of (i) 0, (ii) 5, (iii) 10, (iv) 50 μM ferrocene-acetic acid. (B) Impedance data for this system at equilibrium potential. (C) Nyquist plot with simulation model data (line) and experimental data (dots) for 1 μM and 10 μM ferrocene-acetic acid.

The dimethylaminomethyl-ferrocene "electron shuttle" (Figure 8) is positively charged in neutral aqueous solution with possible implication on reactivity. Voltammetric responses shown in in Figure 8A are consistent with redox mediator activity but with an additional shift in the response and a high peak current at 50 μM dimethylaminomethyl-ferrocene concentration. Voltammetric data in Table 2 suggests that dimethylaminomethyl-ferrocene should be similar in reactivity when compared to ferrocene-dimethanol and therefore the additional anodic current (and the unusually sharp peak shape) may be associated with additional complexity, e.g. favorable interaction with the modified surface or between cationic dimethylaminomethyl-ferrocene and $Fe(CN)_6^{3-/4-}$ at the electrode surface.

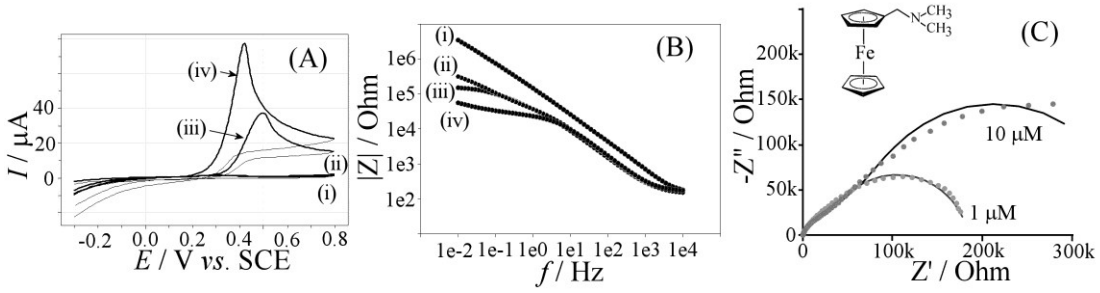

Figure 8. (A) Cyclic voltammograms (scan rate 50 mVs^{-1}) for a 3 mm glassy carbon electrode immersed in aqueous 5 mM $Fe(CN)_6^{3-}$, 5 mM $Fe(CN)_6^{4-}$, and 0.1 M KNO_3 with addition of (i) 0, (ii) 5, (iii) 10, (iv) 50 µM dimethylaminomethyl-ferrocene. (B) Impedance data for this system at equilibrium potential. (C) Nyquist plot with simulation model data (line) and experimental data (dots) for 1 µM and 10 µM dimethylamino-methyl-ferrocene.

Finally, butyl-ferrocene is employed as "electron shuttle" (Figure 9) and similar trends are observed. The solubility of butyl-ferrocene in the aqueous phase is low and at 50 µM nominal concentration clearly additional anodic activity is seen in Figure 9A (a sharp peak) due to aggregation at the electrode surface. It is likely that at lower butyl-ferrocene concentration accumulation of the more lipophilic redox probe into the Kolliphor®EL film occurs to further aid the "electron shuttle" process.

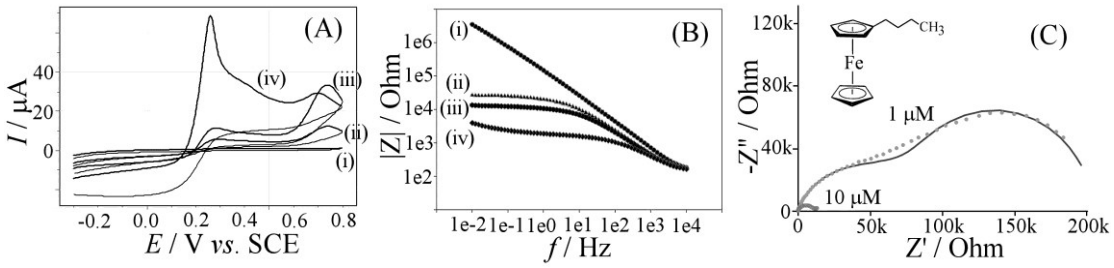

Figure 9. (A) Cyclic voltammograms (scan rate 50 mVs^{-1}) for a 3 mm glassy carbon electrode immersed in aqueous 5 mM $Fe(CN)_6^{3-}$, 5 mM $Fe(CN)_6^{4-}$, and 0.1 M KNO_3 with addition of (i) 0, (ii) 5, (iii) 10, (iv) 50 µM butyl-ferrocene. (B) Impedance data for this system at equilibrium potential. (C) Nyquist plot with simulation model data (line) and experimental data (dots) for 1 µM and 10 µM butyl-ferrocene.

Based on the qualitative comparison of "electron shuttle" efficiency, it appears likely that improved mediator effects are linked to (i) ferrocene derivatives with higher rate of electron transfer across the Kolliphor®EL layer and (ii) ferrocene derivatives with the ability to bind or aggregate at the Kolliphor®EL surface. A more detailed investigation of the underlying mechanism is presented next.

3.3. Kolliphor®EL Grafting Affecting Heterogeneous Electron Transfer Kinetics: Mechanism

The equivalent circuit describing the "electron shuttle" mechanism reasonably closely is shown in Figure 10. The solution resistance R_{sol} and the resistance for heterogeneous electron transfer to the ferrocene derivative R_{et} are complemented with a "short" Warburg impedance to represent at least in first approximation the $Fe(CN)_6^{3-/4-}$ redox system feeding electrons into the layer, and a constant phase element (CPE) is employed to cope with non-ideal capacitive behavior (due to pores and heterogeneity at the surface). The short Warburg impedance is acceptable as a description of the mechanism here as long as the concentration of $Fe(CN)_6^{3-/4-}$ is not perturbed thereby resulting in additional diffusion contributions. This condition is valid only for low ferrocene concentrations and it seems to give reliable results only for dimethylaminomethyl-ferrocene and butyl-ferrocene (*vide infra*).

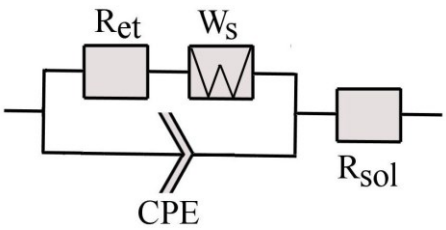

Figure 10. Schematic drawing of the equivalent circuit associated with the modified electrode in contact to the solution.

Data summarized in Table 2 describes the results from quantitative impedance data fitting (see Figures 5C to 9C). It can be observed that the R_{sol} value changes insignificantly and the capacitance C also remains similar to the value observed for the bare glassy carbon electrode. R_{et} appears to be in the kΩ range without clear trend attributable to the structure of ferrocene derivatives. An interesting parameter is W_T, which for the "short" Warburg element is linked to the apparent diffusion layer thickness $\delta_{app} = (W_T \times D)^{1/2}$ (with $D = 0.6 \times 10^{-9}$ m^2s^{-1} here estimated for the ferrocene derivatives[20]). When inspecting the apparent diffusion layer thickness δ_{app}, it is obvious that all values from 41 μm to 486 μm are considerably bigger than the thickness of the Kolliphor®EL film grafted onto the electrode. Therefore diffusion of ferrocene and ferricenium may occur well within the solution phase (see Figure 2). Some of the δ_{app} values are considerable, which suggests that another type of physical process (such as slow bimolecular electron transfer or an additional heterogeneous electron transfer) could be hidden within the data. It is interesting also that although the first three ferrocene derivatives show a *decrease* in δ_{app} with higher mediator concentration, the following two, dimethylaminomethyl-ferrocene and butyl-ferrocene, show an *increase* in δ_{app} with ferrocene concentration. The increase is expected when considering a stronger perturbation of the $Fe(CN)_6^{3-/4-}$ concentration, however, the decrease again suggests another type of physical process underlying the overall process. These trends are also observed in the corresponding data for 5 μM and 50 μM ferrocene mediator (not shown).

For the three more soluble ferrocenes (ferrocene-dimethanol > ferrocene-acetonitrile > ferrocene-acetic acid) a clear trend of lower δ_{app} for more efficient electron shuttling

is seen (see for comparison voltammetry data). The most effective electron shuttle here appears to be dimethylaminomethyl-ferrocene with the smallest diffusion length $\delta = 41$ μm at 1 μM concentration. It is likely that this is linked to some binding of the "electron shuttle" to the Kolliphor®EL film and an indication that in future for this type of ferrocene even lower mediator concentrations are effective.

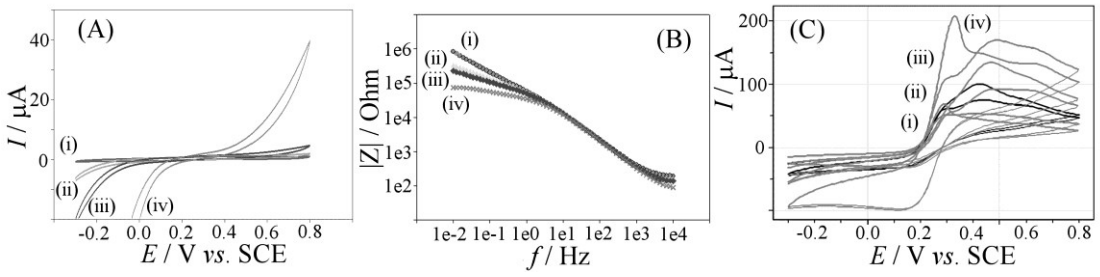

Figure 11. (A) Cyclic voltammograms (scan rate 50 mVs-1) for a 3 mm glassy carbon electrode immersed in aqueous (i) 5, (ii) 10, (iii) 20, (iv) 50 mM $Fe(CN)_6^{3-}$ and $Fe(CN)_6^{4-}$ in 0.1 M KNO_3. (B) Impedance data for the same system at equilibrium potential. (C) Cyclic voltammograms in the presence of 50 μM butylferrocene and with varying $Fe(CN)_6^{3-/4-}$ concentration.

Finally, the effect of the $Fe(CN)_6^{3-/4-}$ redox system in the aqueous phase is assessed. Figure 11A shows data for a Kolliphor®EL modified electrode immersed in solutions of (i) 5, (ii) 10, (iii) 20, (iv) 50 mM each of $Fe(CN)_6^{3-}$ and $Fe(CN)_6^{4-}$. The increase in the rate of electron transfer provides evidence for the first-order nature of the heterogeneous electron transfer. Impedance data in Figure 11B further demonstrate this effect. Finally, in the presence of 50 μM butyl-ferrocene "electron shuttle" an increase in the current response and change in peak shape are seen (Figure 11C) consistent with the voltammetric responses at high mediator concentration being (i) first order in $Fe(CN)_6^{3-/4-}$ and (ii) now in part $Fe(CN)_6^{3-/4-}$ diffusion controlled.

4. Conclusion

Kolliphor®EL has been shown to form mono-layer films on glassy carbon when an anodic grafting protocol is applied. Given the ability of Kolliphor®EL to carry guest species, it is shown here for the first time that guest ferrocene derivatives can be employed to transport electrons across the Kolliphor®EL mono-layer. For a range of ferrocene "electron shuttle" systems a comparison and kinetic analysis were conducted and shuttle efficiencies were evaluated. For all systems the anodic process appears to be considerably faster compared to the cathodic process (causing apparent irreversibility) in line with ferrocenes generally being oxidized at more positive potentials compared to $Fe(CN)_6^{3-/4-}$. The key parameters affecting the "electron shuttle" effect are (i) binding or aggregation ability predominantly based on hydrophobicity and (ii) ability to penetrate the Kolliphor®EL film with faster heterogeneous electron transfer. At low concentration especially butylferrocene and dimethylaminomethyl-ferrocene are highly effective.

In future, a wider range of "electron shuttle" systems could be evaluated in particular with the aim of detecting very low concentrations of redox-active molecules (drugs, bio-markers, pollutants). It will be interesting to explore lower concentrations and more hydrophobic mediator systems.

Acknowledgements

C.E.H. thanks the University of Bath for a Ph.D. scholarship. K.N. thanks LUT for financial support.

References

(1) Mandler, D.; Kraus-Ophir, S. Self-assembled Monolayers (SAMs) for Electrochemical Sensing. *J. Solid State Electrochem*. **2011**, *15* (7-8), 1535-1558.

(2) Liu, J.Q.; Liu, Z.; Barrow, C.J.; Yang, W.R. Molecularly Engineered Graphene Surfaces for Sensing Applications: A review. *Anal. Chim. Acta* **2015**, *859*, 1-19.

(3) Ates, M.; Sarac, A.S. Conducting Polymer Coated Carbon Surfaces and Biosensor Applications. *Prog. Org. Coat.* **2009**, *66* (4), 337-358.

(4) Murray, R.W. Chemically Modified Electrodes. *Acc. Chem. Res.* **1980**, *13* (5), 135-141.

(5) Gooding, J.J. Advances in Interfacial Design Sensors: Aryl Diazonium Salts for Electrochemical Biosensors and for Modifying Carbon and Metal Electrodes. *Electroanalysis* **2008**, *20* (6), 573-582.

(6) Allongue, P.; Delamar, M.; Desbat, B.; Fagebaume, O.; Hitmi, R.; Pinson, J.; Saveant, J.M. Covalent Modification of Carbon Surfaces by Aryl Radicals Generated from the Electrochemical Reduction of Diazonium Salts. *J. Am. Chem. Soc.* **1997**, *119* (1), 201-207.

(7) Decreau, R.A.; Collman, J.P.; Hosseini, A. Electrochemical Applications. How Click Chemistry Brought Biomimetic Models to the Next Level: Electrocatalysis under Controlled Rate of Electron Transfer. *Chem. Soc. Rev*., **2010**, *39* (4), 1291-1301.

(8) Abiman, P.; Wildgoose, G.G.; Crossley, A.; Jones, J.H.; Compton, R.G. Contrasting pKa of Protonated Bis(3-aminopropyl)-terminated Polyethylene

Glycol "Jeffamine" and the Associated Thermodynamic Parameters in Solution and Covalently Attached to Graphite Surfaces. *Chem. - Eur. J.* **2007**, *13* (34), 9663-9667.

(9) Chow, E.; Gooding, J.J. Peptide Modified Electrodes as Electrochemical Metal Ion Sensors. *Electroanalysis* **2006**, *18* (15), 1437-1448.

(10) Belanger, D.; Pinson, J. Electrografting: a Powerful Method for Surface Modification. *Chem. Soc. Rev.* **2011**, *40* (7), 3995-4048.

(11) Maeda, H.; Saka-iri, Y.; Ogasawara, T.; Huang, C.Z.; Yamauchi, Y.; Ohmori, H. Anodization in Oligo(ethylene glycol) as an Initial Derivatization Tool for Preparing Glassy Carbon Electrodes Covalently Modified with Amino Compounds: Effective Access to a 2,2,6,6-Tetramethylpiperidinyl-1-oxyl (TEMPO)-Modified Glassy Carbon Electrode. *Chem. Pharm. Bull.* **2001**, *49* (10), 1349-1351.

(12) Maeda, H.; Itami, M.; Katayama, K.; Yamauchi, Y.; Ohmori, H. Anodization of Glassy Carbon Electrodes in Oligomers of Ethylene Glycol And their Monomethyl Ethers as a Tool for the Elimination of Protein Adsorption. *Anal. Sci.* **1997**, *13* (5), 721-727.

(13) Maeda, H.; Kitano, T.; Huang, C.Z.; Katayama, K.; Yamauchi, Y.; Ohmori, H. Effective Method for the Covalent Introduction of the 2-(2-Carboxymethoxyethoxy)ethoxy Group on a Glassy Carbon Electrode by Anodization in Triethylene Glycol. *Anal. Sci*. **1999**, *15* (6), 531-536.

(14) Hotchen, C.E.; Maybury, I.J.; Nelson, G.W.; Foord, J.S.; Holdway, P.; Marken, F. Amplified Electron Transfer at Poly-Ethylene-Glycol (PEG) Grafted Electrodes. *Phys. Chem. Chem. Phys.* **2015**, *17*, 11260-11268.

(15) Maeda, H.; Yamauchi, Y.; Hosoe, M.; Li, T.X.; Yamagichi, E.; Kasamatsu, M.; Ohmori, H. Direct Covalent Modification of Glassy Carbon Surfaces with 1-Alkanols by Electrochemical Oxidation. *Chem. Pharm. Bull.* **1994**, *42* (9), 1870-1873.

(16) Gelderblom, H.; Verweij, J.; Nooter, K.; Sparreboom, A. Chremophor EL: the Drawbacks and Advantages of Vehicle Selection for Drug Formulation. *Eur. J. Cancer* **2001**, *37* (13), 1590-1598.

(17) Ishihara, H. Current Status and Prospects of Polyethyleneglycol-Modified Medicines. *Biol. Pharm. Bull.* **2013**, *36* (6), 883-888.

(18) Barnes, E.O.; Lewis, G.E.M.; Dale, S.E.C.; Marken, F.; Compton, R.G. Generator-Collector Double Electrode Systems: A review. *Analyst* **2012**, *137* (5), 1068-1081.

(19) Wang, X.Y.; Pang, G.C. Amplification Systems of Weak Interaction Biosensors: Applications and Prospects. *Sens. Rev.* **2015**, *35* (1), 30-42.

(20) Si, Y.M.; Sun, Z.Z.; Zhang, N.; Qi, W.; Li, S.Y.; Chen, L.J.; Wang, H. Ultrasensitive Electroanalysis of Low-Level Free microRNAs in Blood by Maximum Signal Amplification of Catalytic Silver Deposition using Alkaline Phosphatase-Incorporated Gold Nanoclusters. *Anal. Chem.* **2014**, *86* (20), 10406-10414.

(21) Wagner, C.D.; Davis, L.E.; Zeller, M.V.; Taylor, J.A.; Raymond R.M.; Gale, L.H. *Surf. Interface Anal.* **1981**, *3*, 211 and are used here from Appendix 6 of "Practical Surface Analysis", Vol. 1., 2nd Edition, by C. D. Wagner, eds. D. Briggs and M.P. Seah, Published by J. Wiley and Sons in 1990, ISBN 0-471-92081-9.

(22) Ferro, S.; Dal Colle, M.; De Battisti, A. Chemical Surface Characterization of Electrochemically and Thermally Oxidized Boron-Doped Diamond Film Electrodes. *Carbon* **2005**, *43* (6), 1191-1203.

(23) Schlapak, R.; Caruana, D.; Armitage, D.; Howorka, S. Semipermeable Poly(ethyleneglycol) Films: the Relationship Between Permeability and Molecular Structure of Polymer Chains. *Soft Matter* **2009**,*5*, 4104-4112.

(24) Xiong, L.H.J.; Batchelor-McAuley, C.: Ward, K.R.; Downing, C.; Hartshorne, R.S.; Lawrence, N.S.; Compton, R.G. Voltammetry at Graphite Electrodes: The Oxidation of Hexacyanoferrate (II) (Ferrocyanide) does not Exhibit Pure Outer-Sphere Electron Transfer Kinetics and is Sensitive to Pre-Exposure of the Electrode to Organic Solvents, *J. Electroanal. Chem*. **2011**, *661* (1), 144-149.

(25) French, R.W.; Collins, A.M.; Marken, F. Growth and Application of Paired Gold Electrode Junctions: Evidence for Nitrosonium Phosphate During Nitric Oxide Oxidation. *Electroanalysis* **2008**, *20* (22), 2403-2409.

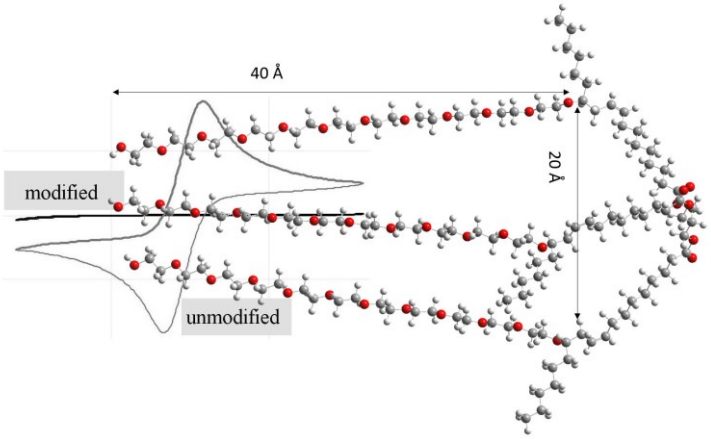

Graphical Abstract: